Journal of Colloid and Interface Science 575 (2020) 326–336

Contents lists available at ScienceDirect

Journal of Colloid and Interface Science

journal homepage: www.elsevier.com/locate/jcis

Hansen solubility parameters obtained via molecular dynamics simulations as a route to predict siloxane surfactant adsorption

Daniël P. Faasen [a,1], Ahmed Jarray [b,1], Harold J.W. Zandvliet [a], E. Stefan Kooij [a], Wojciech Kwiecinski [a,*]

[a] Physics of Interfaces and Nanomaterials Group, MESA+ Institute for Nanotechnology, University of Twente, P.O. Box 217, 7500 AE Enschede, the Netherlands
[b] Multi Scale Mechanics (MSM), MESA+ Institute for Nanotechnology, University of Twente, P.O. Box 217, 7500 AE Enschede, the Netherlands

HIGHLIGHTS

- Surfactant molecules adsorb on a silicon substrate which has a detrimental effect on ink-jet printing.
- Solubility parameter is computed using molecular dynamics simulations.
- The effect of the solvent and the surface properties on surfactant adsorption are investigated.
- Surfactant adsorption on solid surfaces can be predicted by the Hansen solubility parameters.

GRAPHICAL ABSTRACT

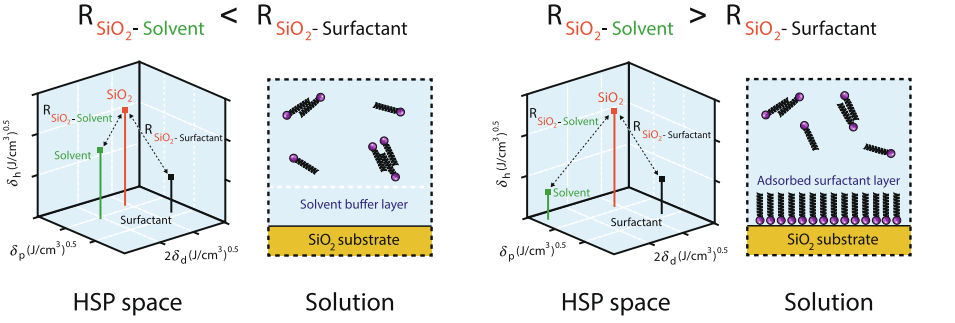

ARTICLE INFO

Article history:
Received 20 January 2020
Revised 17 April 2020
Accepted 17 April 2020
Available online 27 April 2020

Keywords:
Wetting
Surfactants
Adsorption
Solubility parameter
Intermolecular interaction
Inkjet printing

ABSTRACT

Hypothesis: The Hansen Solubility Parameters (HSP) derived from Molecular Dynamics (MD) simulations can be used as a fast approach to predict surfactants adsorption on a solid surface.

Experiments and simulations: We focused on the specific case of siloxane-based surfactants adsorption on silicon oxide surface (SiO_2), encountered in inkjet printing processes. A simplified atomistic model of the SiO_2 surface was designed to enable the computation of its solubility parameter using MD, and to subsequently determine the interactions of the SiO_2 surface with the siloxane-based surfactant and the various solvents employed. Surfactant adsorption was characterized experimentally using contact angle goniometry, ellipsometry, XPS and AFM.

Findings: Comparison of the numerical results with experiments showed that the HSP theory allows to identify the range of solvents that are likely to prevent surfactant adsorption on the SiO_2 surface. The proposed approach indicates that polar solvents, such as acetone and triacetin, which are strongly attracted to the silicon oxide surface might form a shield that prevents siloxane-based surfactants adsorption. This simple approach, can guide the selection of adequate solvents for surfaces and surfactants with specific chemical structures, providing opportunities for controlling interfacial adsorption.

1. Introduction

The quality of inkjet printing is closely related to the wettability characteristics of the printhead and the surface tension of the ink. The former has a significant effect on the velocity and shape of the jetted droplets [1], whereas the latter plays a key role in the imbibition and spreading of the ink on the porous substrate [2,3]. This is

* Corresponding author.
E-mail addresses: d.p.faasen@utwente.nl (D.P. Faasen), a.jarray@utwente.nl (A. Jarray), h.j.w.zandvliet@utwente.nl (H.J.W. Zandvliet), e.s.kooij@utwente.nl (E.S. Kooij), w.kwiecinski@utwente.nl (W. Kwiecinski).
[1] These authors contributed equally.

https://doi.org/10.1016/j.jcis.2020.04.070
0021-9797/

why surfactants are often added the ink solutions in order to reduce the surface tension and improve the spreading of the ink droplet [4]. However, surfactants containing siloxane groups (-Si-O-Si-) can adsorb on the nozzle plate, usually made out of silicon, and alter its wettability. This in turn can lead to non-zero jetting angles (i.e., the liquid jet direction is not normal to the nozzle-plate), which may deteriorate the quality of the printed image (see Fig. 1). Another consequence of the dewetting of the silicon oxide is the risk of air bubble entrainment inside the nozzle, which can completely block the jetting process [1]. We anticipate that a more detailed understanding of the underlying molecular interactions that govern the surfactant-substrate adsorption would facilitate the formulation of optimal ink solutions that do not alter the wettability of the nozzle plate.

Siloxane-based surfactants are surface active in both aqueous and non-aqueous media, with a widespread use owing to their low surface tension, low toxicity and synthetically versatile structure [5]. This class of surfactants is commonly used in ink formulations, and in various other applications such as paint, textile, and agriculture [6,7]. In this study, because of its simple molecular structure, we have chosen 3-ethylhepta-methyltrisiloxane (EHTS) as a model for a surfactant containing siloxane groups.

In general, the adsorption of a molecule from bulk solution to the interface is controlled by the molecular structure of the adsorbate as well as the properties of the solvent and the adsorbing surface. Surfactants adsorption on silica has been studied through experiments [8–10] and molecular dynamics simulations [11–13]. Using MD, Zhou et al. [13] showed that the wetting properties of hydroxylated silica are affected by the surfactant alignment in the adsorption layer. Tiberg et al. [8] and later Tummala et al. [11] emphasized on the importance of hydrogen-bonding between oxygen atoms in the surfactant headgroups and surface hydroxyl groups in the adsorption of nonionic surfactants. Similarly, Levresse et al. [14] and Cohen-Addad et al. [15] argued that hydrogen-bonding with Si-OH groups is the driving force for the adsorption of siloxane-based molecules. Alternatively, other studies showed that depending on the adsorbate molecular structure, the adsorption process can be highly affected by the polarity of the solvents [10,16,17] or by the dispersive van der Waals interactions between the adsorbate and the silicon surface [18,19]. Therefore, knowing a priori the specific molecular interactions, namely the polar, dispersive and hydrogen-bonding interactions, that control the adsorption behaviour of the surfactant [20] is required in order to gain a more comprehensive understanding of the adsorption processes, and will help in better selecting and designing surfactants and solvents for specific applications. From this standpoint, the concept of Hansen Solubility Parameters (HSP) [21] (i.e., square root of the Cohesive Energy Density, CED) can be used to quantify these interactions at the molecular level. For the calculation of the solubility parameter, predictive group contribution models have been proposed by several authors [22–24]. However, these semi-empirical models are not reliable for complex structures, such as surfactants and branched polymers [25–27] or complex molecules with long-range electrostatic interactions [28,29]. This is because these models are based on the notion of additivity of property values of the chemical groups (e.g., -CH3 and -OH) of which the molecule is composed, and therefore, they do not account for molecular conformations, and change in molecular structure due variation of temperature. This means that group contributions models cannot distinguish between polymers consisting of the same functional groups, but different molecular structures, and cannot properly account for highly directional interactions, such as hydrogen-bonding and electrostatic interactions that may be affected by the temperature or pressure. It has also been shown that group contribution methods overestimate the hydrogen bonding contribution component of the solubility parameter [27]. As such, Molecular Dynamics (MD) simulation techniques have emerged as a complementary and convenient tool for the prediction of the solubility parameter [30–34].

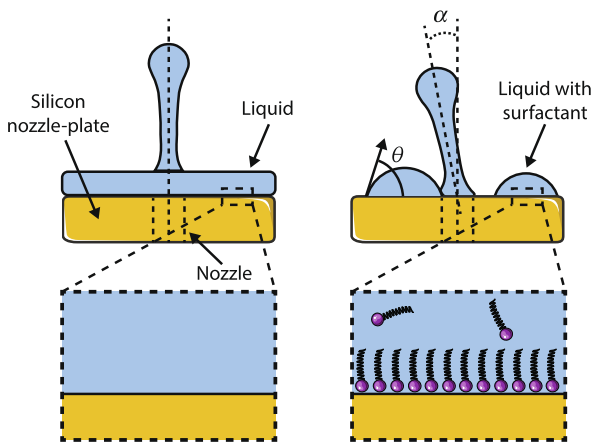

Fig. 1. Schematic of the deposition of EHTS surfactant on the silicon oxide surface of the printhead. The hydrophobic tail of the surfactant changes the wetting properties of the printhead nozzle-plate. Note that, after EHTS adsorption, ink creates sessile droplets on a printhead instead of a continuous film. This may lead to jetting angles $\alpha \neq 0$ if the droplets are close to a nozzle.

The solubility parameter has played a critical role in the screening of solvents [35–38] and the estimation of interactions and incompatibilities between materials [39,40]. Other studies showed that the HSP method can be used for preliminary screening of optimum solvents for aerogels [41], additives in crystallization processes [42], and crude oils for asphalt precipitation [42], thus minimizing time and resource investment. The solubility parameter has also been correlated to a variety of properties such as the surface tension, viscosity, work of adhesion and tensile strength [32,35,37,43,44]. However, the application of HSP's derived from MD to the area of surfactants adsorption onto solid surfaces remains unexplored.

In this paper, we investigate the effect of solvents with various molecular structures and polarities on the amount of EHTS adsorbed on a silicon oxide substrate. We propose an approach for the prediction of this adsorption from the surface-surfactant and solvent-surfactant intermolecular interactions, explaining the subsequent effect it has on the wetting properties of the silicon surface. A combination of experimental and numerical methods were used and compared. On the experimental side, the deposition of the surfactant was studied using contact angle goniometry, ellipsometry and atomic force microscopy. On the numerical side, Hansen solubility parameter values were calculated using MD simulations, where a simplified atomistic model of the silicon surface was used to compute its solubility parameter. These were complemented by MD simulations of solvent-surfactant mixtures to extract the order parameter describing their mixing degree.

2. Materials and methods

2.1. Materials and sample preparation

Methyl benzoate and 2-n-butoxyethyl acetate (BEA) with 99% and 98% purity were obtained from ABCR GmbH. 3-ethylheptamethyltrisiloxane (EHTS) with a purity of 97% was acquired from Fluorochem. The molecular structure of EHTS is shown in Fig. 2. All other chemicals were purchased from Sigma Aldrich with a purity of 99% or higher. A schematic of their molecular structure is provided in the supplementary file. All chemicals were used without any further purification.

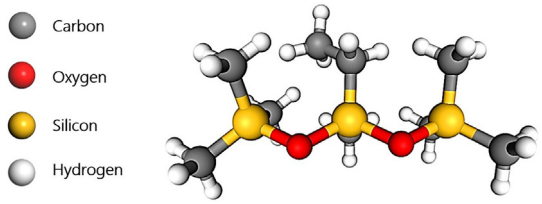

Fig. 2. Molecular structure of 3-ethylheptamethyltrisiloxane (EHTS).

Silicon(100) wafers (Okmetic), diced into 1.5 × 1.5 cm^2 pieces, were used for sample preparation. First, they were cleaned with a piranha solution (3:1 (v/v - volume fraction) of sulfuric acid (Merck, 96%) and hydrogen peroxide (Merch, 30%)) for 15 min. Afterwards, they were rinsed thoroughly with Milli-Q water (resistivity $= 18.2\ M\Omega \cdot cm$) and dried in a nitrogen stream. The piranha cleaning step was performed to remove organic contaminants from the silicon oxide surface, and also to activate the surface chemically by creating silanol (-Si-O-H) and siloxane groups (-Si-O-Si-). Cleaned silicon substrate samples were immediately transferred into a 5ml of a previously prepared solution of choice (various EHTS-solvents mixtures). All EHTS solutions contained 1% weight fraction of the EHTS. Samples were kept in a solution for at least 48 hours in order to simulate long time adsorption behaviour that can be encountered in industrial applications.

After being removed from the EHTS solution, samples were rinsed with acetone in order to remove remnants of the reactive solution. Subsequently, they were placed in a beaker filled with acetone and cleaned in an ultrasonic cleaner for 5 min. Later, samples were rinsed with Milli-Q water and dried in a nitrogen stream. Lastly, the ultrasonic cleaning step was repeated with Milli-Q water.

2.2. Experimental methods

Contact angle Advancing (ACA) and receding contact angles (RCA) were obtained by placing a 1 μL droplet of Milli-Q water on a substrate using a glass syringe (Hamilton) and an automatic dispensing system of a contact angle measurement set-up (OCA15+, DataPhysics Instruments GmbH). Afterwards, the droplet was inflated slowly (0.1 μL/s) to a volume of 2 μL, which was recorded using a CCD camera (pco.pixelfly, PCO AG). Subsequently, 1 μL of liquid was retracted with the same speed and the process was recorded again. The contact angle was obtained from the recordings by fitting a sphere only to the bottom part of a droplet (in order to neglect the deformation caused by the needle) using an in-house Matlab script (2017b version, The MathWorks, Inc.). The ACA was defined as the highest CA observed during droplet inflation and the RCA as the lowest CA during retraction [45]. If the observed ACA for a specific sample was lower than 10°, we assumed that its contact angle is too low to be measured by this method, and complete spreading is considered.

Ellipsometry A VB-400-VASE (J.A. Woollam Co.) ellipsometer was used for layer thickness measurements. The obtained data was analyzed with WVASE32 (J.A. Woollam Co.) software [46]. All samples were measured with light energies $0.8 - 4.5$ eV and $65, 70, 75°$ incident angles. Deposited layer thickness was obtained by creating a model consisting of a Cauchy material on top of a native silicon oxide layer [47]. Native silicon oxide thickness was obtained by measuring a reference sample which was only cleaned with piranha solution and using silicon oxide optical properties from the work of Hirzinger et al. [48]. Cauchy parameters of: A = 1.45, B = 0.1, C = 0, were used for layer thickness fitting.

Atomic force microscopy AFM measurements were performed with a Dimension Icon AFM (Bruker). The obtained force-distance data was processed using in-house Matlab scripts. NSC35 probes (Mikromasch) with a typical tip radius of 8 nm and a spring constant of approximately 6N/m were used for the measurements. The spring constant of a specific cantilever was determined using the thermal tuning procedure prior to the experiments. Topographical maps were obtained using the PeakForce tapping mode.

Cleaning experiments Additional cleaning experiments were performed in order to investigate the possibility of removing the adsorbed layer by using commonly available cleaning chemicals (see Fig. 6 B and C). The cleaning procedure involves the sonication in an ultrasonic bath for 5 min at room temperature with various cleaning chemicals. After each sonication step, the samples were rinsed with Milli-Q water and then dried in a nitrogen stream. Afterwards, the cleaned silicon substrate sample was analyzed with ellipsometry and CA goniometry followed by a next cleaning step of the same sample. Alkaline solutions such as NaOH or KOH were not used because they etch the silicon oxide surface effectively destroying the sample [49]. Alconox is an anionic detergent used for laboratory glass cleaning. Alconox solution was prepared by dissolving 12 g of powder (purchased from Sigma Aldrich) in 1 L of demi-water.

2.3. Hansen Solubility Parameter (HSP) theory

The solubility parameter describes the intermolecular interactions of a pure substance. It is a measure of the total cohesive forces holding the molecules together in a given liquid or an amorphous solid. The solubility parameter of a compound is equal to the square root of its cohesive energy density, CED, which is defined as the ratio of the energy of vaporization, ΔU_{vap} to the molar volume, V_m [50,51],

$$\delta = \sqrt{CED} = \sqrt{\frac{\Delta U_{vap}}{V_m}} = \sqrt{\frac{\Delta H_{vap} - RT}{V_m}}, \tag{1}$$

where ΔH_{vap} is the molar enthalpy of vaporization, R is the gas constant ($8.31\ J \cdot mol^{-1} \cdot K^{-1}$), and T the temperature. This Hildebrand definition of the solubility parameter was initially intended for non-polar and non-associating systems. To overcome this limitation, Crowley et al. [52] and later Hansen [36] proposed to split this parameter into three components,

$$\delta = \sqrt{\delta_d^2 + \delta_p^2 + \delta_h^2}, \tag{2}$$

where δ_d is the dispersive component, δ_p is the polar component, and δ_h represents the hydrogen-bonding component of the solubility parameter. The dispersive interactions are related to the non-covalent London forces resulting from the instantaneous fluctuations of electrons. The polar interactions originate from the permanent dipoles in the molecules. Molecules which have an asymmetrical distribution of charges among its atoms will have a high solubility parameter polar component. The hydrogen bonding component of the solubility parameter describes the highly directional attraction occurring between a specific hydrogen atom from one molecule and another acceptor atom from a second molecule. Based on this division of the solubility parameter, Hansen developed the Hansen Solubility Parameter (HSP) 3D space (see Fig. 3), in which every material is represented by a single point corresponding to the geometric sum of the Hansen solubility parameter components. Two liquids, A and B, having close positions in this 3D space are likely to have high interactions and should be miscible when mixed. Similarly, dissolution is favored when the solubility parameters of the solvent match those of the solute in the Hansen 3D space. The solubility parameter distance, $R_{a(A-B)}$, between the positions of two substances in the 3D-HSP diagram was defined by Hansen [36] as:

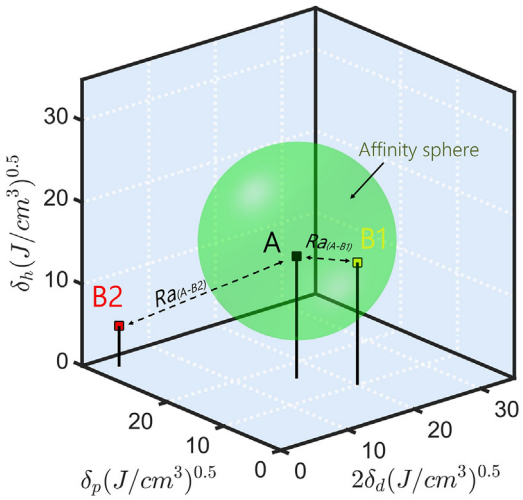

Fig. 3. Schematic representation of the 3D Hansen solubility parameters space. Here $R_{a(A-B1)} > R_{a(A-B2)}$, indicating that material A has stronger interactions with material B1 than with B2.

$$R_{a(A-B)} = \sqrt{4(\delta_{d,A} - \delta_{d,B})^2 + (\delta_{p,A} - \delta_{p,B})^2 + (\delta_{h,A} - \delta_{h,B})^2}. \quad (3)$$

Here, the scaling factor "4" was suggested by Hansen based on empirical testing because it correctly represented the solubility data as an affinity sphere encompassing the good solvents [36]. This sphere contains the liquids which exhibit high miscibility (or solubility) with a particular solute. The center of the sphere represents the solute coordinates (i.e., the three solubility parameter components of the solute), and the radius of the sphere corresponds to the largest R_a distance of the set of liquids miscible (or have high affinity) with the solute. In this work, $R_{a(A-B)}$ will give information on the solvents-surfactant and solvents-silicon interactions, i.e., R_a and R_{ss}, will henceforth refer, respectively, to the distances between the solvents and the surfactant and between the solvent and the silicon substrate in the Hansen space.

2.4. Molecular dynamics simulations

2.4.1. Hydroxilated silicon dioxide model

Hydroxilated silicon dioxide is a solid material composed of a non-interacting bulk silicon layer and SiOH interface (i.e., the reactive siloxane surface), making the determination of the solubility parameter by conventional CED calculation or group contribution methods not possible [53,54]. Another issue is that the interaction with the solvent or the surfactant occurs at a well-defined interface and not at the bulk silicon layer of the substrate. A typical experimental approach for deriving the solubility parameter of solid surfaces is by measuring the solubility parameter of solvents with close molecular properties to the solid interface [53–58]. But still, this does not provide the actual solubility parameter value of the surface of the material. In this work, rather than looking for similar compounds that match the surface energy of the interface, we designed a simplified model molecule with similar atomistic structure as the hydroxilated silicon surface. Then, its solubility parameter was computed using MD as the debundling energy of one of its interfacial fragments, where each fragment represents a simplified polymer-like model consisting of a finite number of repeating units of silane and siloxane groups (Si-OH) as shown in Fig. 4. The fragment model contains all the interacting atoms at the interface of the hydroxilated silicon dioxide substrate, which ensure comparable intermolecular interactions. A similar molecular model that reproduces the main characteristics of a hydroxylated silicon dioxide surface was also proposed by Tielens et al. [59] and Perez-Beltran et al. [60]. Although, 8 repeating units with 4 fragments in the simulation box are sufficient to compute the solubility parameter [39,61,62], our simulation was performed with an ensemble consisting of 20 fragments, where each fragment contains 8 repetitions units, and each unit has 4 siloxane groups. Other simplified models of silicon dioxide with different terminal groups, namely dehydrated silicon surface and amorphous silicon oxide, were also tested (see supplementary files), however, we found that a hydroxilated silicon dioxide model gives the best results.

2.4.2. Computation of the solubility parameter

For the computation of the solubility parameter, molecular dynamics simulations were performed using LAMMPS [63]. We chose to use the DERIDING [64] forcefield since it describes explicitly the hydrogen-bonding interactions. Molecules were first packed in a 3-D simulation cell with periodic boundary conditions. DERIDING [64] forcefield was applied to the periodic model and energy minimization was performed. Then, simulations were run for 200 ps with a time step of 1 fs. The temperature was set at T = 298 K and controlled by a Nose-Hoover thermostat. Long range electrostatics were described using the charge equilibration (Qeq) method of Rappé and Goddard [65]. A cut-off distance of 10 Å smoothed at 11 Å was used for van der Waals and Couloumb interactions. Ewald summation with an accuracy of 0.001 kcal/mol was used to calculate the Coulombic interactions. Since the hydrogen-bonding term is short-ranged, it was truncated at 3.5 Å and smoothly shifted to 0 kcal/mol at 4.5 Å, along with an angle cutoff of 120° to limit the scope of the DERIDING hydrogen bonding potential.

The cohesive energy density is the total amount of internal energy per mole per unit volume of a substance arising from all of the intermolecular interactions that hold the molecules together (i.e., the energy required to separate all molecules in a unit volume of liquid). This energy was computed by averaging the intermolecular non-bonded energy over the last 20 ps of the resulting molecular trajectories:

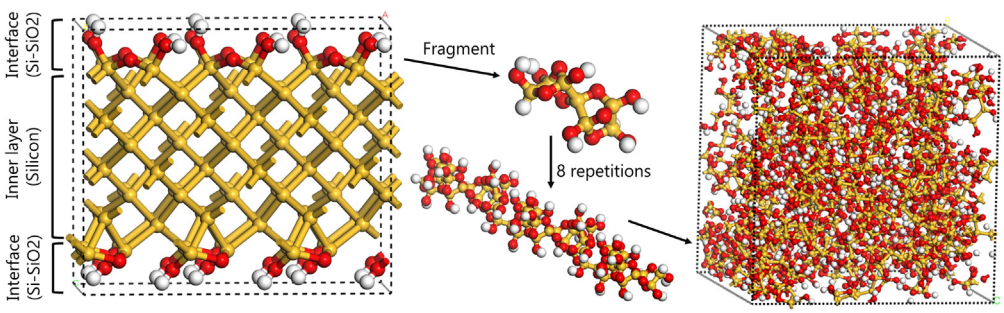

Fig. 4. Simplified molecular model of hydroxilated silicon dioxide used for the calculation of the solubility parameter.

$$\delta_k = \sqrt{\frac{-\langle \sum_{i=1}^{n} E_{Inter,k,i} \rangle}{N_{av} V}}, \quad (4)$$

with n the number of molecules in the simulation cell, N_{av} the Avogadro number, k runs over the total energy, van der Waals energy, and Coulomb energy, respectively. "$\langle\ \rangle$" denotes a time average over the duration of the simulation, V the simulation box volume, the index i refers to the energy of the molecule i, and the index c represents the total energy of the molecules in the simulation box. The hydrogen-bonding component of the solubility parameter was then obtained using Eq. (2).

2.4.3. Surfactant-solvent mixing

Molecular dynamic simulations of surfactant-solvents mixing were also carried out to complement the solubility parameter results. Molecules of solvents and surfactants (50–50% v/v - volume fraction) were packed into a tetragonal simulations box, where periodic boundary conditions were applied in all three directions. Following the energy minimization step, MD simulations were conducted using the DERIDING forcefield for 5 ns in the canonical thermodynamic NVT ensemble at T = 298 K, with 1 fs time-step, where the experimental density of the mixtures was used to generate a simulation cell dimensions of 6 × 6 × 2.5 nm^3. For a better visualization of the surfactant-solvent phase separation, the concentration field was interpolated from the positions of the atoms that compose each molecule in the fluid mixtures [66,67] (see Fig. 5) using a Gaussian data interpolation of radius 5 Å.

The order parameter, P, which has many equivalent definitions [68,69], is a quantitative measure of the degree of mixing. In our simulations, it was averaged from the resulting MD simulations concentration fields over the last 500 ps. The order parameter of the surfactant $P_{\text{surfactant}}$ is defined as the volume average of the difference between the local and the overall volume fraction squared of the surfactant in the mixture [68]:

$$P_{\text{surfactant}} = \frac{1}{V} \int^{V} (\eta^2_{\text{surfactant}}(r) - \eta^2_{\text{surfactant}}) dr, \quad (5)$$

where $\eta_{\text{surfactant}}$ is the volume fraction of the surfactants (i.e., dimensionless local concentration) and V the volume of the simulation box. High values of the order parameter indicate phase separation, while small values are indicative of mixing between the surfactant and the solvent.

3. Results and discussion

EHTS solution in hexane (1% w/w) was prepared in order to mimic ink containing surfactant with siloxane groups. Fig. 6 (A) displays the change in wetting properties with time of the piranha-cleaned silicon substrate which was placed in an EHTS solution. Water, which initially ($t = 0$) wets the untreated silicon substrate, starts to display a finite contact angle and contact angle hysteresis after a sample was placed in the EHTS solution for only 15 min. After approximately 4 hours, the wetting properties of the sample stabilize. We did not measure any increase in the water contact angle even after two weeks. This change in wettability of the silicon substrate may affect the jetting of the ink from the nozzle as shown in Fig. 1.

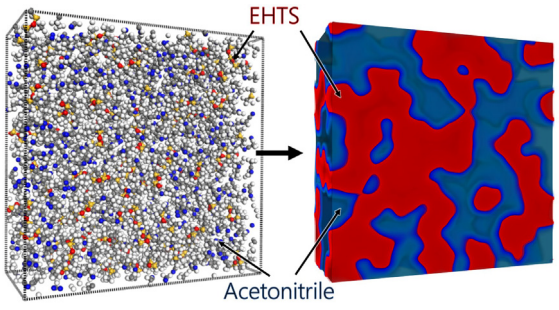

Fig. 5. MD simulation of EHTS-acetonitrile mixing (left) and corresponding concentration field of the binary fluid (right).

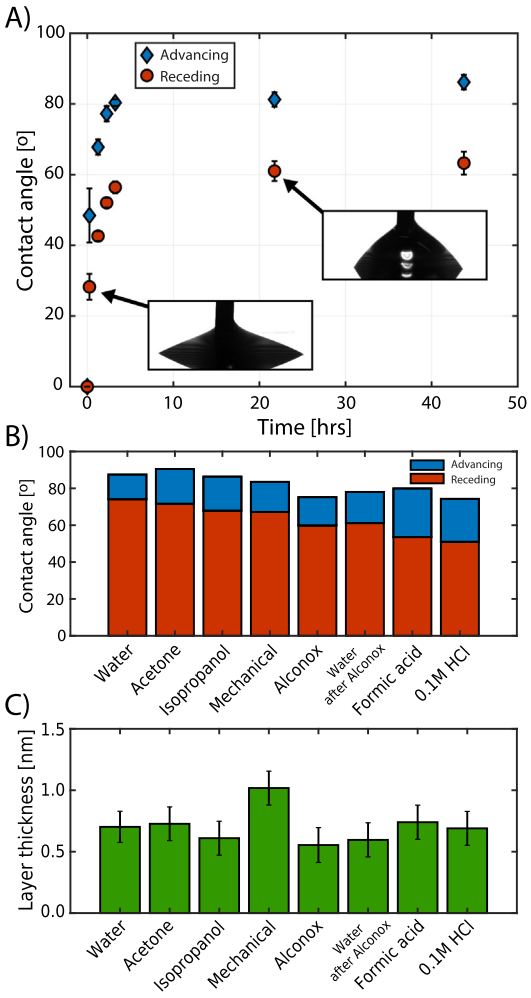

Fig. 6. (A) Advancing and receding contact angles of water versus time spent by the silicon substrate in a 1%(w/w) EHTS-hexane solution. Note that after the first few hours the wetting properties of the sample remain stable. (B) Advancing and receding contact angles of pure water and, (C) layer thickness measured with ellipsometry on the sample stored for 48 hours in EHTS solution in hexane after various cleaning steps. Cleaning steps are shown in a chronological order from left to right. Error bars on the plots display a standard deviation.

In an attempt to restore the original wetting properties of the silicon oxide surface treated with EHTS solution, we tried using various organic and inorganic solvents and cleaning chemicals (see Fig. 6 (B) and (C)). The chosen cleaning procedures are meant to mimic the cleaning that could be easily applied to the operating machine parts (such as an inkjet printhead) in order to restore the wetting properties similar to those of a clean silicon oxide. We would like to recall that altered wetting properties of the silicon surface may disrupt the jetting process in case of inkjet printing (see Fig. 1).

We could observe a slight decrease in advancing and receding contact angles of water after treating the surface with Alconox solution as well as formic and hydrochloric acids. In general

however, the applied cleaning steps did not significantly impact the wetting properties of the silicon substrate. Furthermore, the thickness of the deposited layer measured with ellipsometry remains constant within the error bars. Only after mechanical cleaning we noted a modest increase in the measured layer thickness, which we attribute to the additional unwanted remnants that might have been transferred onto the surface during the wiping process. These experimental observations show that the wetting properties of a silicon surface can be swiftly and significantly altered by a solution containing siloxane-based chemicals. Furthermore, the surface cannot be restored to its original state by using conventional and commonly available chemical cleaning procedures, suggesting that EHTS adsorbs to the surface by chemical bonding rather than physisorption.

In order to verify the mechanism of adsorption, the silicon oxide surface topography was characterized with an AFM in a clean state and after EHTS adsorption. Topographical scans of both surfaces show flat surfaces with RMS roughnesses of 247 pm and 250 pm for clean and EHTS-modified surface, respectively (see Figs. 7(A) and (B)). However, force-spectroscopy measurements (insets in Figs. 7(A) and (B)) reveal significant differences between these surfaces. Clean silicon oxide surfaces display large adhesion forces between the tip and the surface, as well as a short range of interactions. Surface modification with EHTS resulted in a substantial decrease of adhesion forces and large increase in interaction distance during retraction, which we attribute to adsorbed EHTS molecules. Therefore, we conclude that the silicon oxide surface, after the reaction with EHTS, is covered with a very thin, molecular layer, which does not affect the surface roughness. This result is further supported by the small layer thickness obtained by the ellipsometry measurements (Fig. 6 (C)) and is typical for the chemisorption. Additionally, XPS measurements (for details, see supplementary information) revealed that samples treated with pure EHTS and its solution in hexane displayed an additional Silicon Si-2p peak with a binding energy of approximately 102 eV,

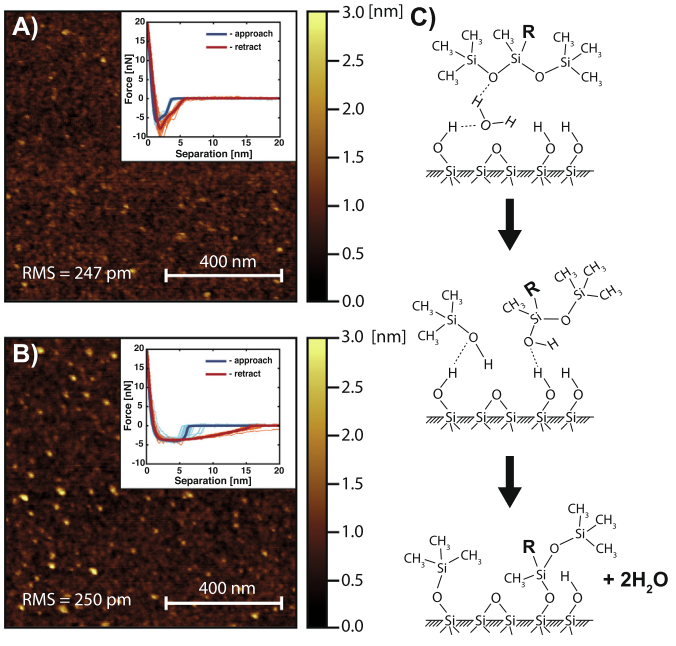

Fig. 7. $1 \times 1\ \mu m^2$ topographical maps of clean silicon oxide surface (A) and the surface treated with EHTS (B). Inserts on panels (A) and (B) show 40 force spectroscopy measurements (thin lines) and the median of those measurements (thick lines). (C) Sketch of the chemical reaction leading to the chemisorption of molecules containig trisiloxane group to the silicon oxide surface. For the EHTS molecule the end group R is (-CH2-CH3). The dotted lines indicate hydrogen bonds.

typically associated with silane bonds (-Si-O-Si-) [16], which we attribute to the EHTS adsorption on a surface (see Fig. S3 in the SI). Analysis of the C-1s peaks (i.e., carbon atoms) also showed that compared to the amount of Si, significantly more carbon atoms are present on the surface treated with EHTS (see Fig. S4 in the SI). Furthermore, survey spectrum showed that no unexpected elements were found on the surface (see Fig. S2 in the SI).

A schematic representation of the chemical reaction of molecules containing a trisiloxane group (such as EHTS) with the silicon oxide surface is shown in Fig. 7 (C), based on studies done previously for poly(dimethyl-siloxanes) [70]. Note that, as sketched in Fig. 7 (C), the reaction is facilitated by the presence of water. However, it should be mentioned that the reaction was also found to occur between fully dehydrated silicon oxide substrates and siloxane compound solutions, although with lower rates [70]. Nevertheless, in Ref. [70] the authors calcinated silicon oxide substrate at very high temperatures and provided reaction solutions through a complicated dehydration procedure in order to make sure that they are entirely dry. Because such measures were not taken in our samples preparation procedure and because it is necessary to heat silicon oxide to high temperatures in order to dehydrate it [71,72], we can safely assume that a small amount of water will always be present on the hydrophilic, piranha cleaned substrate. Therefore, in our experimental conditions we anticipate that the chemisorption reaction will occur with the participation of water.

3.1. Influence of surfactant-solvent interactions

One way to prevent changes of the wetting properties by the host fluid, observed in Fig. 6, is by changing the solvent in which the surfactant is dissolved. Fig. 8 (A) displays how water droplets behave on silicon samples treated with 1% w/w EHTS solutions created with three organic solvents with vastly different chemical structures and properties, namely: furan, acetone, and hexane. When the surface is treated with hexane-EHTS solution, water forms a sessile droplet indicating partial wetting, as opposed to a full spreading obtained for a clean silicon oxide as it was already shown in Fig. 6 (A). However, the contact angle observed when the surface is treated with acetone-EHTS solution is much smaller, and full spreading of water happens when it is treated with EHTS-furan solution, indicating that the silicon surface was hardly affected by these solutions. In order to study this phenomena, we prepared samples with EHTS solutions in various organic solvents. ACA and RCA of silicon surfaces affected by those solutions as well as pure solvents for comparison are presented in Fig. 8 (B). In order to investigate solvent-surfactant interactions systematically, solvents were ordered according to their solubility distance relative to the surfactant (R_a) in the Hansen parameter space. The larger R_a, the higher the intermolecular interactions between the solvent and the surfactant. The solubility parameters used here were calculated using molecular dynamics simulations and are presented in Table 1. ACA and RCA plotted against numerical values of R_a can be found in Fig. A1 in the appendix. The high hydrogen bonding components of the hydroxilated silicon substrate as shown in Table 1 suggests that hydrogen-bonds between EHTS's hydrogen atoms and the siloxane groups of the surface may contribute to EHTS adsorption. This is in line with previous studies [11,15,73] reporting on the importance of hydrogen-bonding in the adsorption of molecules containing oxygen atoms on silicon oxide surface.

It is clear from Fig. 8 (B) that non-polar solvents such as decane or hexane, with the smallest R_a to EHTS, result in the most substantial change of the wetting properties of a silicon substrate. Furthermore, for the same non-polar solvents, the thickest layer was measured by ellipsometry (Fig. 8 (C)). However, the surfactant solutions in many other solvents have little effect on the wetting

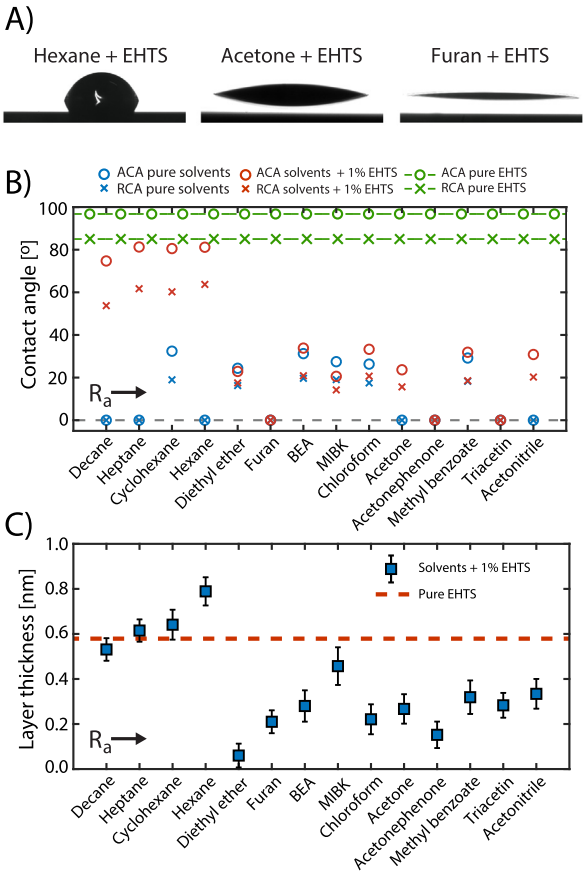

Fig. 8. (A) Snapshots of water droplets on a substrate treated with 1% (w/w) EHTS solutions in furan, acetone and hexane. Note the droplets display significantly different contact angles. (B) ACA and RCA of water on a silicon surface treated with EHTS solutions (1% w/w) in different solvents (red marks). Solvents were ordered based on their R_a relative to EHTS in Hansen parameter space. Blue symbols show the ACA and RCA of water measured on substrates submerged in pure solvent for reference. Green symbols display ACA and RCA measured for a substrate treated with pure EHTS. (C) Layer thickness obtained using ellipsometry measurements on a silicon substrate after treating them with EHTS solutions using the same sorting as in (B). Red dashed line marks the layer thickness measured for a substrate submerged in pure EHTS. (For interpretation of the references to color in this figure legend, the reader is referred to the web version of this article.)

Table 1
Solubility parameter components in $(J/cm^3)^{0.5}$ for EHTS surfactant, hydroxilated silicon oxide, and the various solvents used in this study.

Compound	δ_{Total}	δ_d	δ_p	δ_h
Acetone	20.16	16.19	11.99	0.74
Acetonephenone	22.65	20.47	9.65	0.94
Acetonitrile	22.23	15.44	15.99	0.31
BEA	20.47	17.99	9.76	0.35
Chloroform	21.73	18.73	11.01	0.40
Cyclohexane	17.87	17.84	1.09	0.16
Decane	17.01	16.96	1.27	0.29
Diethylether	17.04	15.41	7.24	0.69
EHTS[a]	17.00	16.90	1.40	0.40
Furan	20.53	18.26	9.37	0.51
Heptane	16.14	16.10	1.09	0.33
Hexane	15.58	15.51	1.20	0.86
MethylBenzoate	22.63	20.20	10.19	0.49
MIBK	20.02	16.54	11.28	0.00
Triacetin	22.72	18.35	13.39	0.43
Hydroxilated silicon oxide[b]	37.54	19.80	27.26	16.56

BEA: Methyl benzoate, EHTS: 3-ethylheptamethyltrisiloxane, MIBK: Methyl isobutyl ketone.
[a] Surfactant.
[b] Oxidized printhead plate surface.

properties of the silicon dioxide (like acetone or acetonitrile for instance), or they did not affect them at all (e.g., furan or triacetin). Note that in case of some solvents, like acetone or chloroform, treating a substrate with pure solvents already increased water contact angles (blue symbols in Fig. 8 (B)), which can be attributed to physisorption of those solvents on highly polar silicon oxide surface. Nonetheless, all solvents formed transparent and stable solutions with EHTS. This is also reflected by the values of R_a which are all below 15 (see Fig. A1 in the Appendix), indicating that all the solutions prepared are well mixed. Mixing is a necessary condition to prevent surfactant adsorption, otherwise, phase separation occurs and pushes the surfactant molecules to the interface. To confirm this, we performed MD simulations of the mixing of EHTS-solvent (50–50% v/v) solutions and we computed the order parameter. The latter represents a quantitative measure of the degree of surfactant-solvent mixing and is shown in Fig. 9 (A). Large order parameter translates into phase separation and low surfactant-solvent affinity. Water is used here as a reference solvent to illustrate a complete phase separation case.

The evolution of the order parameter of the mixing of EHTS surfactant with water and with cyclohexane are shown in Fig. 9 (A) along with the MD simulations snapshots at 0, 500 and 5000 ps. Red and blue areas correspond to EHTS and solvents, respectively. When using water as a solvent, which is a highly polar molecule that can exhibit strong hydrogen-bonding interactions, demixing is observed. This leads to a complete phase separation. In contrast,

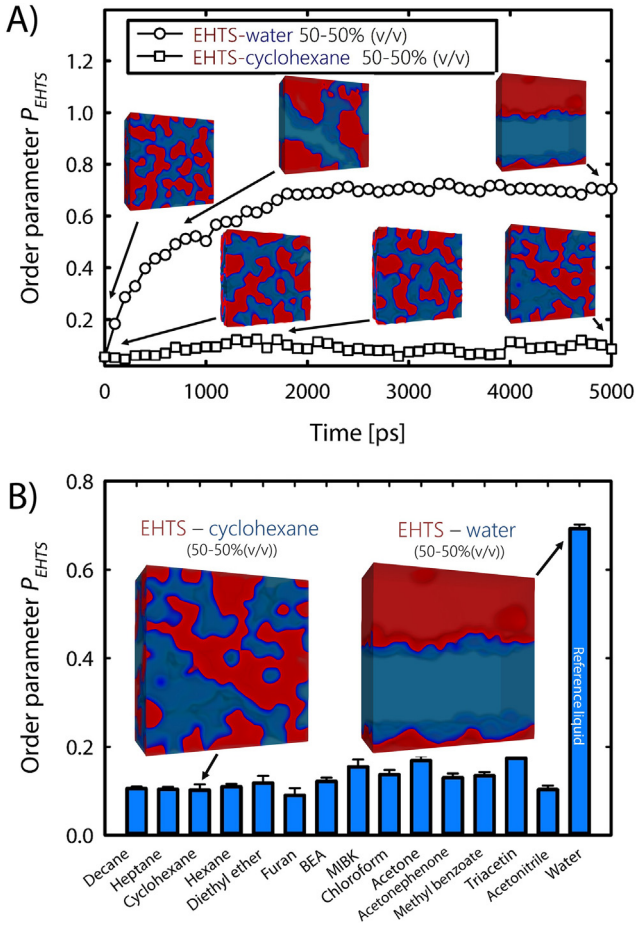

Fig. 9. MD simulation of EHTS-solvents mixing. (A) Order parameter as a function of simulation time of the mixing of EHTS-water and EHTS-cyclohexane (50–50%(v/v)). Simulation snapshots were taken at 0, 500 and 5000 ps. (B) Order parameter of the various EHTS-solvent mixtures, and water is used as a reference liquid to illustrate an unmixed system.

as the simulation progresses, the order parameter of EHTS when mixed with cyclohexane remains low compared to the EHTS-water solution, indicating a mixed system. This is reflected by the average order parameter values shown in Fig. 9 (B), with a low P_{EHTS} = 0.11 for EHTS-cyclohexane and a high P_{EHTS} = 0.82 for EHTS-water solution. All the other solvents used in this study show low values of the order parameter, below 0.2, which confirms that all the EHTS-solvent solutions perfectly mix. However, the influence of solvents still does not fully explain the observed immediate transition to lower layer thicknesses and contact angles with the increase of R_a (see Fig. 8). For this reason and because the solvent should not only dissolve the surfactant, but also prevent its interaction with the surface, it is necessary to consider the surface-solvent interactions to correctly predict surfactant adsorption. The evolution of the order parameter versus simulation time of all the solvents is shown in the supplementary file along with the MD simulation snapshots of the remaining EHTS-solvent mixing.

3.2. Influence of surface-solvent interactions

Historically, HSP were designed as a tool to systematically investigate the miscibility and solubility of chemical entities. However, the adsorption of a surfactant from a solution is influenced not only by its interactions with the solvent, but also by its interactions with the surface of the substrate. In order to quantify surface-liquid interactions, the HSP parameters of the silicon surface were calculated using molecular dynamics simulations as described in subsection 2.4. MD simulations give a total solubility parameter of hydroxilated silicon dioxide equal to 37.54 $(J/cm^3)^{0.5}$ which is interestingly close to that of silicon dioxide (35.3 $(J/cm^3)^{0.5}$) obtained from experimental liquid-solid chromatography data by Row [56].

The ACA and RCA values of water on silicon surface and the measured layer thicknesses, ordered based on the increasing solvent-surface distance (R_{ss}) in the HSP space, are presented in Figs. 10 (A) and (B), respectively. Because the piranha cleaning procedure, followed by rinsing with Milli-Q water leaves the majority of the surface terminated with hydroxyl (-OH) groups, the solubility parameters calculated for the maximally hydroxylated silicon oxide model were used in Fig. 10 (A). The data plotted against numerical values of solvent-surface distances R_{ss} are presented in Fig. A2 of the Appendix. R_{ss} values were calculated using Eq. (3), where component "A" is the surface of the substrate and component "B" is the solvent.

Note that, the solvent order in Fig. 10 has changed and, in contrast to the previous R_a solvent-surfactant based sorting (Fig. 8), the non-polar solvents are now in the right part of the plot. This is intuitive since piranha cleaning leaves silicon oxide surface terminated mostly with polar hydroxyl groups which will attract polar solvents, like acetone, resulting in high solvent-surface affinity. However, this is not the case for non-polar solvents, like hexane, which do not have any polar groups in their molecular structure. This could indicate that polar solvents which are strongly attracted to the silicon oxide surface might shield it from the EHTS. Surprisingly, the EHTS-surface HSP distance plotted with black dashed line in Fig. 10 falls exactly where the sharp transition between the presence and the lack of surfactant adsorption occurs. This implies that if the EHTS has higher affinity towards the surface than the solvent, it will react with the termination groups present on silicon oxide surface, forming a coating layer and permanently alter the wetting properties of the surface. These predictions results also indicate that polar solvents, such as furan and triacetin, which have high molecular cohesive interactions and high affinity to the surface, can effectively prevent the formation of hydrogen-bonds between the surfactant and the silicon substrate. Formation

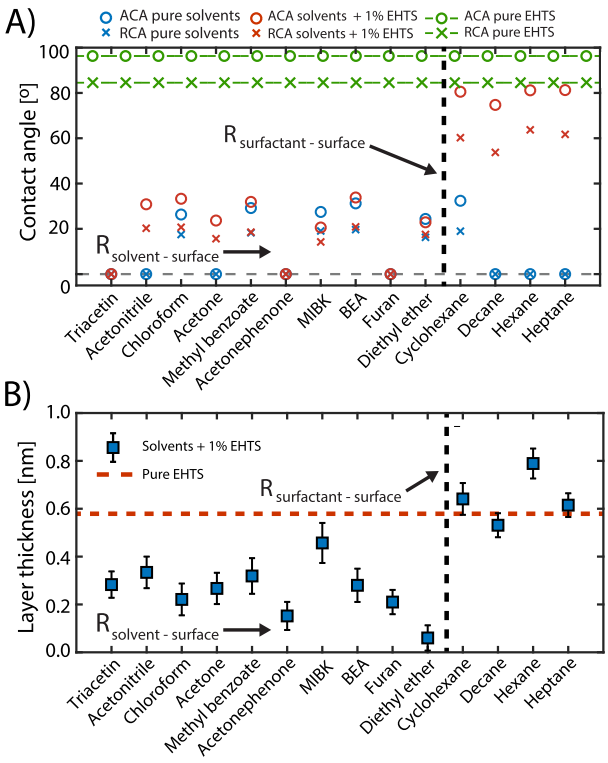

Fig. 10. (A) ACA and RCA of water on a silicon surface treated with EHTS solutions (1% w/w) in different solvents (red marks). Solvents were ordered based on their distance from the surface in HSP space. Black dashed line shows the distance between the EHTS surfactant and the surface in the HSP. Blue symbols show the ACA and RCA of water measured on substrates submerged in pure solvent for reference. Green symbols display ACA and RCA measured for a substrate treated with pure EHTS. (B) Layer thickness obtained with ellipsometry measurements on a silicon substrates after treating them with EHTS solutions using the same sorting as in (A). Red dashed line marks the layer thickness measured for a substrate submerged in pure EHTS. (For interpretation of the references to color in this figure legend, the reader is referred to the web version of this article.)

of hydrogen-bonds is a major factor affecting non-ionic surfactant adsorption, as shown by several studies [8,11,14,15]. This infers that the hydrogen bonds formed between the polar solvents and the silanol groups on the surface effectively prevents the chemisorption of EHTS.

In this study, two other silicon dioxide simplified models were tested. The first model is not hydroxylated and only contains siloxane (Si-O-Si) groups, and the second model is 50% hydroxilated (i.e., terminated with 50% (-OH) and 50% (Si-O-Si) groups). However, only the maximally hydroxilated silicon oxide model, whose structure is expected to be the closest to the silicon dioxide substrate obtained from our sample preparation method, resulted in perfect matching with experiments (see Figures S2, S3 and S4 in the supplementary file). The deviations observed for the two other surface terminations highlight the importance of precise knowledge of surface chemistry for a proper use of this predictive method.

4. Conclusions

We successfully utilized a novel method based on Hansen Solubility Parameters (HSP) to characterize the interactions between surfactant solutions and a silicon oxide (SiO_2) surface, and predict the adsorption of a siloxane-based surfactant (EHTS). The calculation of the solubility parameters of the silicon oxide surface, which is not possible by traditional group contribution methods [22–24,54], was done by computing the cohesive energy of a model

fragment of SiO_2 using molecular dynamics simulations. The method's predictions were confirmed by ellipsometry, XPS and wetting experiments, and showed that siloxane-based surfactant adsorption can be reduced by a proper selection of solvents, depending on the surface-surfactant molecular interactions. Solvents with a HSP distance relative to the surface lower than that of the surfactant are likely to prevent surfactant adsorption.

The main advantage of this approach relies on its simplicity, as it is based on the molecular structure of the molecules, and does not require experimental inputs or fitted data. Compared to conventional experimental tools for measuring surfactant adsorption on solid surfaces [74–77], the proposed approach is cost-efficient, fast and provides complementary insights into the adsorption mechanism in terms of the intermolecular interactions of the materials involved. This can significantly reduce the tedious and time-consuming trial-and-error type experiments, when searching for adequate solvents and surfactants with respect to their adsorption on a given surface [16–18], facilitating for instance the development of better inks [1]. Furthermore, the predictive approach is not limited to surfactants, but can also be applied to the adsorption of other chemicals, relevant for many industrial applications, including pharmaceutics [78], oil production [18,79] and agriculture [80,81]. However, the HSP approach cannot unveil all the subtleties of the surfactants adsorption process, as it gives predictions based on the intermolecular interactions of pure substances, and only accounts for the direct contact energies between them. Consequently, it does not provide information on the surfactant arrangement on the interface and cannot capture effects associated with the formation of hydrogen-bonds over time. It would therefore be interesting to perform MD simulations to illustrate the behavior of siloxane surfactant-solvent mixtures on the vicinity of silicon oxide surface in order to obtain additional insights into the adsorption process.

CRediT authorship contribution statement

Daniel P. Faasen: Writing – original draft, Investigation, Data curation. **Ahmed Jarray:** Writing – original draft, Writing – review and editing, Investigation, Methodology, Software. **Harold J.W. Zandvliet:** Funding Acquisition, Resources, Supervision. **E. Stefan Kooij:** Supervision, Methodology, Writing – review and editing. **Wojciech Kwieciński:** Conceptualization, Methodology, Writing – original draft, Writing – review and editing, Investigation.

Declaration of Competing Interest

The authors declare that they have no known competing financial interests or personal relationships that could have appeared to influence the work reported in this paper.

Acknowledgements

This work is part of an Industrial Partnership Programme of the Foundation for Fundamental Research on Matter (FOM), which is financially supported by the Netherlands Organisation for Scientific Research (NWO). This research program is co-financed by Océ Technologies B.V., University of Twente, and Eindhoven University of Technology.

Additionally, we would like to thank all members of the FIP program for useful discussions and all their suggestions. Especially, we would like to acknowledge Marc van der Berg and Björn Ketelaars who greatly contributed to setting up this project. We also thank Stefan Luding and Wouter K. den Otter for their help and advices. We would also like to acknowledge Gerard Kip for helping with the XPS measurements.

Appendix A

Figs. A1 and A2 show the advancing and receding contact angles of water on silicon dioxide surface treated with various EHTS-solvent solutions, plotted against the EHTS-solvent (R_a) and the solvent-surface ($R_{solvent-surface}$) distances, respectively.

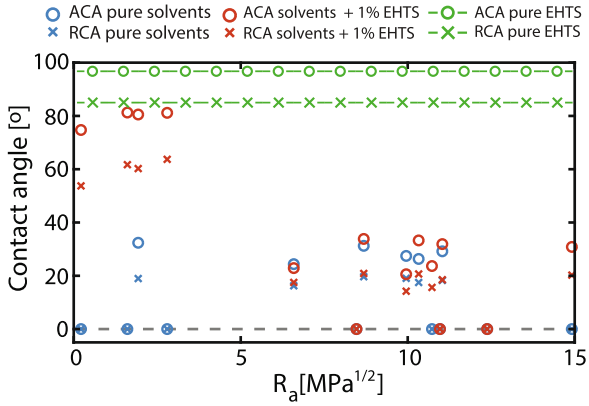

Fig. A1. ACA and RCA of water on a silicon surface treated with EHTS solutions (1% w/w) in different solvents (red marks), as a function of R_a of solvents from EHTS in Hansen parameter space. Blue symbols show the ACA and RCA of water measured on substrates submerged in pure solvent for reference. Green symbols display ACA and RCA measured for a substrate treated with pure EHTS. (For interpretation of the references to color in this figure legend, the reader is referred to the web version of this article.)

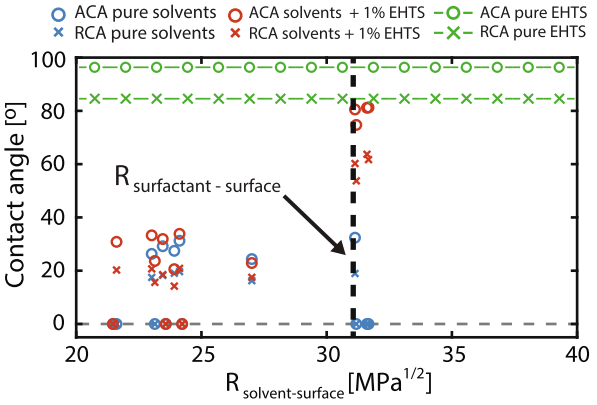

Fig. A2. ACA and RCA of water on a silicon surface treated with EHTS solutions (1% w/w) in different solvents (red marks), as a function of distance of solvents from the surface in HSP space. Black dashed line shows the distance between the EHTS surfactant and the surface in HSP. Blue symbols show the ACA and RCA of water measured on substrate submerged in pure solvent for reference. Green symbols display ACA and RCA measured for a substrate treated with pure EHTS. (For interpretation of the references to color in this figure legend, the reader is referred to the web version of this article.)

Appendix B. Supplementary material

Supplementary data associated with this article can be found, in the online version, at https://doi.org/10.1016/j.jcis.2020.04.070.

References

[1] Herman Wijshoff, The dynamics of the piezo inkjet printhead operation, Phys. Rep. 491 (4–5) (2010) 77–177.
[2] B.-J. De Gans, Paul C Duineveld, Ulrich S Schubert, Inkjet printing of polymers: state of the art and future developments, Adv. Mater. 16 (3) (2004) 203–213.

[3] A. Clarke, T.D. Blake, K. Carruthers, A. Woodward, Spreading and imbibition of liquid droplets on porous surfaces, Langmuir 18 (8) (2002) 2980–2984.
[4] Stephen D Hoath, Fundamentals of inkjet printing: the science of inkjet and droplets, John Wiley & Sons, 2016.
[5] Ian Donald Robb, Specialist surfactants. Springer Science & Business, Media (2012).
[6] R.M. Hill, Silicone Surfactants, Marcel Dekker, 1999.
[7] Joachim Venzmer, Superspreading – 20 years of physicochemical research, Curr. Opinion Colloid Interface Sci. 16 (4) (2011) 335–343.
[8] Fredrik Tiberg, Bengt Joensson, Ji-an Tang, Bjoern Lindman, Ellipsometry studies of the self-assembly of nonionic surfactants at the silica-water interface: equilibrium aspects, Langmuir 10 (7) (1994) 2294–2300.
[9] Santanu Paria, Kartic C. Khilar, A review on experimental studies of surfactant adsorption at the hydrophilic solid–water interface, Adv. Colloid Interface Sci. 110(3) (2004) 75–95.
[10] Eugène Papirer, Adsorption on Silica Surfaces, vol. 90, CRC Press, 2000.
[11] Naga Rajesh Tummala, Liu Shi, Alberto Striolo, Molecular dynamics simulations of surfactants at the silica–water interface: anionic vs nonionic headgroups. J. Colloid Interface Sci. 362(1) (2011) 135–143.
[12] James S Smith, Oleg Borodin, Grant D Smith, Edward M Kober, A molecular dynamics simulation and quantum chemistry study of poly (dimethylsiloxane)–silica nanoparticle interactions, J. Polym. Sci., Part B: Polym. Phys. 45 (13) (2007) 1599–1615.
[13] Peng Zhou, Jian Hou, Youguo Yan, Jiqian Wang, The effect of surfactant adsorption on surface wettability and flow resistance in slit nanopore: A molecular dynamics study, J. Colloid Interface Sci. 513 (2018) 379–388.
[14] P. Levresse, D.L. Feke, I. Manas-Zloczower, Analysis of the formation of bound poly (dimethylsiloxane) on silica, Polymer 39 (17) (1998) 3919–3924.
[15] Jean-Pierre Cohen-Addad, Philippe Huchot, Philippe Jost, Alain Pouchelon, Hydroxyl or methyl terminated poly (dimethylsiloxane) chains: Kinetics of adsorption on silica in mechanical mixtures, Polymer 30 (1) (1989) 143–146.
[16] G. Jakša, B. Štefane, J. Kovač, Influence of different solvents on the morphology of aptms-modified silicon surfaces, Appli. Surface Sci. 315 (2014) 516–522.
[17] V.K. Pogorelyi, V.N. Barvinchenko, E.M. Pakhlov, O.V. Smirnova, The effect of solvent nature on the adsorption interaction between cinnamic acid and silicon dioxide, Colloid J. 67 (2) (2005) 172–176.
[18] Yong Xiong, Tiantian Cao, Qian Chen, Zhen Li, Yue Yang, Xu. Shengming, Shiling Yuan, Johan Sjoblom, Xu. Zhenghe, Adsorption of a polyaromatic compound on silica surfaces from organic solvents studied by molecular dynamics simulation and afm imaging, J. Phys. Chem. C 121 (9) (2017) 5020–5028.
[19] H. Barthel, E. Nikitina, Ins and ir study of intermolecular interactions at the fumed silica-polydimethylsiloxane interphase, part 3. sicica-siloxane adsorption complexes, Silicon Chem. 1 (4) (2002) 261–279.
[20] P. Somasundaran, L. Huang, Adsorption/aggregation of surfactants and their mixtures at solid–liquid interfaces, Adv. Colloid Interface Sci. 88 (1–2) (2000) 179–208.
[21] J.H. Hildebrand, R.L. Scott, The Solubility of Nonelectrolytes, vol. 3, , Reinhold Pub, 1950.
[22] D.W. Vankreve, Chemical structure and properties of coal. 28. coal constitution and solvent extraction, Fuel 44 (4) (1965) 229.
[23] Jean-Pierre Hansen, Loup Verlet, Phase transitions of the lennard-jones system, Phys. Rev. 184(1) (1969) 151.
[24] K.L. Hoy, New values of the solubility parameters from vapor pressure data, J. Paint Technol. 42 (541) (1970) 76–118.
[25] Phillip Choi, Tom A. Kavassalis, Alfred Rudin, Estimation of hansen solubility parameters for (hydroxyethyl) and (hydroxypropyl) cellulose through molecular simulation. Ind. Eng. Chem. Res. 33(12) (1994) 3154–3159.
[26] Mitesh R. Shah, Ganapati D. Yadav, Prediction of sorption in polymers using quantum chemical calculations: application to polymer membranes, J. Mem. Sci. 427 (2013) 108–117.
[27] Martina Levin, Per Redelius, Determining the hansen solubility parameter of three corrosion inhibitors and the correlation with mineral oil, Energy Fuels 26 (12) (2012) 7243–7250.
[28] M. Langer, M. Höltje, Nora Anne Urbanetz, B. Brandt, H.-D. Höltje, B.C. Lippold, Investigations on the predictability of the formation of glassy solid solutions of drugs in sugar alcohols, Int. J. Pharmaceutics 252(1–2) (2003) 167–179.
[29] Jasmine Gupta, Cletus Nunes, Shyam Vyas, Sriramakamal Jonnalagadda, Prediction of solubility parameters and miscibility of pharmaceutical compounds by molecular dynamics simulations, J. Phys. Chem. B 115 (9) (2011) 2014–2023.
[30] John L Lewin, Katie A Maerzke, Nathan E Schultz, Richard B Ross, J. Ilja Siepmann, Ilja Siepmann. Prediction of hildebrand solubility parameters of acrylate and methacrylate monomers and their mixtures by molecular simulation, J. Appl. Polym. Sci. 116 (1) (2010) 1–9.
[31] Xianping Chen, Cadmus Yuan, Cell K.Y. Wong, Guoqi Zhang, Molecular modeling of temperature dependence of solubility parameters for amorphous polymers, J. Mol. Model. 18 (6) (2012) 2333–2341.
[32] Ahmed Jarray, Vincent Gerbaud, Mehrdji Hémati, Prediction of solid–binder affinity in dry and aqueous systems: Work of adhesion approach vs. ideal tensile strength approach, Powder Technol. 271 (2015) 61–75..
[33] Yamini Sudha Sistla, Lucky Jain, Ashok Khanna, Validation and prediction of solubility parameters of ionic liquids for co2 capture, Separ. Purif. Technol. 97 (2012) 51–64.
[34] Ahmed Jarray, Herman Wijshoff, Jurriaan A. Luiken, Wouter den Otter, Systematic approach for wettability prediction using molecular dynamics simulations. Soft Matter (2020) (in press). doi: 10.1039/D0SM00197J.
[35] R.F. Fedors, D.W. Van Krevelen, P.J. Hoftyzer, Handbook of Solubility Parameters and Other Cohesion Parameters, CRC, 1983.
[36] Charles M. Hansen, The Three Dimensional Solubility Parameter, vol. 14. 1967.
[37] D.M. Koenhen, C.A. Smolders, The determination of solubility parameters of solvents and polymers by means of correlations with other physical quantities, J. Appl. Polym. Sci. 19 (4) (1975) 1163–1179.
[38] Yaocihuatl Medina-Gonzalez, Ahmed Jarray, Séverine Camy, Jean-Stéphane Condoret, Vincent Gerbaud, Co 2-expanded alkyl lactates: A physicochemical and molecular modeling study, J. Solution Chem. 46 (2) (2017) 259–280.
[39] Ahmed Jarray, Vincent Gerbaud, Mehrdji Hemati, Polymer-plasticizer compatibility during coating formulation: A multi-scale investigation, Prog. Org. Coat. 101 (2016) 195–206.
[40] K. Adamska, A. Voelkel, M. Sandomierski, Characterization of mesoporous aluminosilicate materials by means of inverse liquid chromatography, J. Chromatogr. A (2019) 460544.
[41] Zhiyuan Zhu, Geert MBF Snellings, Matthias M Koebel, Wim J Malfait, Superinsulating polyisocyanate based aerogels: a targeted search for the optimum solvent system, ACS Appl. Mater. Interfaces 9 (21) (2017) 18222–18230.
[42] Guangpu Liu, Thomas B Hansen, Qu. Haiyan, Mingshi Yang, Jari P Pajander, Jukka Rantanen, Lars P Christensen, Crystallization of piroxicam solid forms and the effects of additives, Chem. Eng. Technol. 37 (8) (2014) 1297–1304.
[43] Charles M Hansen, 50 years with solubility parameters–past and future, Prog. Org. Coat. 51 (1) (2004) 77–84.
[44] Yu. Weiyan, Wanguo Hou, Correlations of surface free energy and solubility parameters for solid substances, J. Colloid Interface Sci. 544 (2019) 8–13.
[45] T. Huhtamäki, X. Tian, J.T. Korhonen, R.H.A. Ras, Surface-wetting characterization using contact-angle measurements, Nat. Protoc. 13 (7) (2018) 1521–1538.
[46] J.A. Woollam, Guide to using wvase32, JA Woollam, 2002.
[47] Hiroyuki Fujiwara, Spectroscopic Ellipsometry, John Wiley & Sons, 2007.
[48] C.M. Herzinger, B. Johs, W.A. McGahan, J.A. Woollam, W. Paulson, Ellipsometric determination of optical constants for silicon and thermally grown silicon dioxide via a multi-sample, multi-wavelength, multi-angle investigation, J. Appl. Phys. 83 (6) (1998) 3323–3336.
[49] M.A. Gos lvez, R.M. Nieminen, Surface morphology during anisotropic wet chemical etching of crystalline silicon, New J. Phys. 5 (2003) 100–100.
[50] J.H. Hildebrand, R.L. Scott, The Solubility of Nonelectrolytes, 1950, Reinhold, New York, 1964.
[51] Joel H Hildebrand, Dipole attraction and hydrogen bond formation in their relation to solubility, Science 83 (2141) (1936) 21–24.
[52] James D Crowley, G.S. Teague, Jr, and Jack W Lowe Jr. A three-dimensional approach to solubility, J. Paint Technol. 38 (496) (1966) 269–280.
[53] Charles M. Hansen, Surface characterization using hansen solubility (cohesion) parameters, in: B.F. Sorensen, L.P. Mikkelsen, H. Lilholt, S. Goutianos, F.S. Abdul-Mahdi (Eds.), Proceedings of the 28th Riso International symposium on materials science: Interface design of polymer matrix composites–mechanics, chemistry, modeling and manufacturing, Riso National Laboratory, Roskilde, Denmark, 2007, pp. 191–197.
[54] Yenny Hernandez, Mustafa Lotya, David Rickard, Shane D Bergin, Jonathan N Coleman, Measurement of multicomponent solubility parameters for graphene facilitates solvent discovery, Langmuir 26 (5) (2009) 3208–3213.
[55] Malcolm E Schrader, George I Loeb, Modern approaches to wettability, Plenum, New York, 1992.
[56] R.C. Rowe, Interactions in the ternary powder system microcrystalline cellulose, magnesium stearate and colloidal silica–a solubility parameter approach, Int. J. Pharmaceutics 45 (3) (1988) 259–261.
[57] Sofie Gårdebjer, J. Martin Andersson, P Restorp Engström, M. Persson, Anders Larsson, Using hansen solubility parameters to predict the dispersion of nano-particles in polymeric films, Polym. Chem. 7 (9) (2016) 1756–1764.
[58] Dong Rag Son, Anjanapura V. Raghu, Kakarla R. Reddy, Han Mo Jeong, Compatibility of thermally reduced graphene with polyesters, J. Macromol. Sci. Part B 55(11) (2016) 1099–1110.
[59] Frederik Tielens, Christel Gervais, Jean François Lambert, Francesco Mauri, Dominique Costa, Ab initio study of the hydroxylated surface of amorphous silica: A representative model, Chem. Mater. 20 (10) (2008) 3336–3344.
[60] Saul Perez-Beltran, Gustavo E. Ramírez-Caballero, Perla B. Balbuena, First-principles calculations of lithiation of a hydroxylated surface of amorphous silicon dioxide, J. Physi. Chem. C 119(29) (2015) 16424–16431.
[61] M. Belmares, M. Blanco, W.A. Goddard Iii, R.B. Ross, G. Caldwell, S.-H. Chou, J. Pham, P.M. Olofson, Cristina Thomas, Hildebrand and hansen solubility parameters from molecular dynamics with applications to electronic nose polymer sensors, J. Comput. Chem. 25 (15) (2004) 1814–1826.
[62] Sheetal S. Jawalkar, Susheelkumar G. Adoor, Malladi Sairam, Mallikarjuna N. Nadagouda, Tejraj M. Aminabhavi, Molecular modeling on the binary blend compatibility of poly (vinyl alcohol) and poly (methyl methacrylate): an atomistic simulation and thermodynamic approach, J. Phys. Chem. B 109(32) (2005) 15611–15620.
[63] Steve Plimpton, Fast parallel algorithms for short-range molecular dynamics, J. Comput. Phys. 117 (1) (1995) 1–19.
[64] Stephen L Mayo, Barry D Olafson, William A Goddard, Dreiding: a generic force field for molecular simulations, J. Phys. chem. 94 (26) (1990) 8897–8909.

[65] Anthony K Rappe, William A Goddard III, A Goddard III. Charge equilibration for molecular dynamics simulations, J. Phys. Chem. 95 (8) (1991) 3358–3363.
[66] Will J Schroeder, Bill Lorensen, Ken Martin, The visualization toolkit: an object-oriented approach to 3D graphics, Kitware (2004).
[67] Daniel J Price, Smoothed particle hydrodynamics and magnetohydrodynamics, J. Comput. Phys. 231 (3) (2012) 759–794.
[68] Sheetal S Jawalkar, Tejraj M Aminabhavi, Molecular modeling simulations and thermodynamic approaches to investigate compatibility/incompatibility of poly (l-lactide) and poly (vinyl alcohol) blends, Polymer 47 (23) (2006) 8061–8071.
[69] Linli He, Linxi Zhang, Haojun Liang, The effects of nanoparticles on the lamellar phase separation of diblock copolymers, J. Phys. Chem. B 112 (14) (2008) 4194–4203.
[70] Gabriel Graffius, Frank Bernardoni, Alexander Y. Fadeev, Covalent functionalization of silica surface using "inert" poly(dimethylsiloxanes), Langmuir 30 (49) (2014) 14797–14807.
[71] L.T. Zhuravlev, The surface chemistry of amorphous silica. zhuravlev model, Colloids Surf., A 173 (1) (2000) 1–38.
[72] Yuliang Wang, Marya Lieberman, Growth of ultrasmooth octadecyltrichlorosilane self-assembled monolayers on sio2, Langmuir 19 (4) (2003) 1159–1167.
[73] Evan Spruijt, P.M. Biesheuvel, Wiebe M. de Vos. Adsorption of charged and neutral polymer chains on silica surfaces: The role of electrostatics, volume exclusion, and hydrogen bonding, Phys. Rev. E, 91(1) (2015) 012601.
[74] C. Bellmann, A. Synytska, A. Caspari, A. Drechsler, K. Grundke, Electrokinetic investigation of surfactant adsorption, J. Colloid Interface Sci. 309 (2) (2007) 225–230.
[75] Spencer C. Clark, William A. Ducker, Exchange rates of surfactant at the solid-liquid interface obtained by atr-ftir, J. Phys. Chem. B 107(34) (2003) 9011–9021.
[76] Fang Pan, Lu. Zhiming, Ian Tucker, Sarah Hosking, Jordan Petkov, Jian R Lu, Surface active complexes formed between keratin polypeptides and ionic surfactants, J. Colloid Interface Sci. 484 (2016) 125–134.
[77] Rui Zhang, P. Somasundaran, Advances in adsorption of surfactants and their mixtures at solid/solution interfaces, Adv. Colloid Interface Sci. 123 (2006) 213–229.
[78] Carol A. McCarthy, Robert J. Ahern, Ken J. Devine, Abina M. Crean, Role of drug adsorption onto the silica surface in drug release from mesoporous silica systems, Mol. Pharm. 15 (1) (2018) 141–149.
[79] Tu. Lan, Hongbo Zeng, Tian Tang, Understanding adsorption of violanthrone-79 as a model asphaltene compound on quartz surface using molecular dynamics simulations, J. Phys. Chem. C 122 (50) (2018) 28787–28796.
[80] Anna Derylo-Marczewska, Magdalena Blachnio, Adam Wojciech Marczewski, Malgorzata Seczkowska, Bogdan Tarasiuk, Phenoxyacid pesticide adsorption on activated carbon – equilibrium and kinetics, Chemosphere 214 (2019) 349–360. ISSN 0045–6535.
[81] Yan-Shuo Lai, Shushi Chen, Adsorption of organophosphate pesticides with humic fraction-immobilized silica gel in hexane, J. Chem. Eng. Data 58 (8) (2013) 2290–2301.